Structure and dynamic dielectric behaviour of ferroelectric $[NH_2(CH_3)_2]_3Sb_2Br_9$ (DMABA)

Structure and dynamic dielectric behaviour of ferroelectric [NH$_2$(CH$_3$)$_2$]$_3$Sb$_2$Br$_9$ (DMABA)

J Zaleski†, Cz Pawlaczyk‡, R Jakubas§ and H-G Unruh‖

† Institute of Chemistry, University of Opole, Oleska 48, 45-951 Opole, Poland
‡ Institute of Molecular Physics, Polish Academy of Sciences, Smoluchowskiego 17, 60179 Poznań, Poland
§ University of Wrocław, Faculty of Chemistry, F Joliot-Curie 14, 50383 Wrocław, Poland
‖ Universität des Saarlandes, Fachbereich Physik, 66041 Saarbrücken, Germany

Abstract. The crystal structure of DMABA has been determined at 293 and 180 K. It crystallizes in the monoclinic $P2_1/c$ space group. The structure was refined to $R_1 = 0.0466$ for 1269 independent reflections at 293 K and $R_1 = 0.038$ for 1728 reflections at 180 K. DMABA is isomorphous with the chlorine analogue, DMACA. Its anionic sublattice forms corrugated two-dimensional layers in the bc plane. There are two crystallographically independent, disordered dimethylammonium cations in the crystal structure. One of them occupies cavities inside the polyanionic layers; the other is located between the layers. The temperature dependence of lattice parameters has been determined between 100 and 290 K. The presence of the ferro–paraelectric phase transition at 164 K has been confirmed. The complex dielectric permittivity of DMABA single crystals in the frequency range 100 Hz–10 GHz between 10 K and 300 K has been measured. The dynamic dielectric behaviour of DMABA is found to be determined by the properties of two independent relaxators: a low frequency one ($\sim$1 MHz at T_c) with a critical slowing down of its dynamics and a high frequency one ($\sim$5 GHz), which is thermally activated and contributes to the electric permittivity at least from about 80 K.

1. Introduction

Alkylammonium halogenoantimonates(III) and bismuthates(III) form a large group of molecular–ionic crystals closely related to the perovskite family. The R$_3$Me$_2$X$_9$ subgroup (where R = CH$_3$NH$_3$, (CH$_3$)$_2$NH$_2$, (CH$_3$)$_3$NH, Me = Sb, Bi, X = Cl, Br), which is very interesting from the dielectric point of view, deserves special attention. The crystals with two-dimensional layers of polyanionic Me$_2$X$_9^{3-}$ units, constituting this family, possess the ferroelectric properties in the low temperature phases. The structural phase transitions in these crystals are governed by the ordering of organic cations [1, 2]. The dimethylammonium analogues [(CH$_3$)$_2$NH$_2$]$_3$Sb$_2$Cl$_9$ (DMACA) and [(CH$_3$)$_2$NH$_2$]$_3$Sb$_2$Br$_9$ (DMABA) appear to be isomorphous at room temperature [3]. DMACA crystallizes in monoclinic symmetry, space group $P2_1/c$. In the room temperature phase there are two crystallographically non-equivalent, disordered DMA cations in the asymmetric part of the unit cell; DMA(1) is located about a centre of symmetry inside the polyanionic cavities whereas the DMA(2) is located at the general position between the layers. The dielectric [4] and x-ray [5] studies clearly showed that the continuous ferro–paraelectric phase transition in DMACA at 242 K is connected with a critical slowing down of reorientations of DMA(1) cation located inside the polyanionic cavity. Proton NMR measurements on DMACA confirmed the presence of dynamically inequivalent DMA

Table 1. Crystal data and structure refinement for DMABA.

Identification code		DMABA	
Empirical formula		$[(CH_3)_2NH_2]_3Sb_2Br_9$	
Formula weight		1100.97	
Temperature	293(2) K		180.0(1) K
Wavelength		0.710 73 Å	
Crystal system, space group		Monoclinic, $P2_1/c$	
Unit cell dimensions	$a = 9.986(2)$ Å		$a = 9.821$ Å
	$b = 9.196(2)$ Å		$b = 9.180$ Å
	$c = 14.531(3)$ Å		$c = 14.445$ Å
	$\beta = 95.05(3)°$		$\beta = 95.10°$
Volume	1329.2(5) Å^3		1297.2(5) Å^3
Z, calculated density	2, 2.751 Mg m^{-3}		2, 2.819 Mg m^{-3}
Absorption coefficient	15.555 mm^{-1}		15.940 mm^{-1}
$F(000)$		996	
Crystal size		0.25 mm × 0.2 mm × 0.2 mm	
Index ranges	$0 \leqslant h \leqslant 9$		$0 \leqslant h \leqslant 10$
	$-9 \leqslant k \leqslant 9$		$0 \leqslant k \leqslant 10$
	$-14 \leqslant l \leqslant 14$		$-16 \leqslant l \leqslant 16$
Reflections collected/unique	2391/1269 ($R_{int} = 0.0246$)		1728/1728
Refinement method		Full-matrix least squares on F^2	
Data/restraints/parameters	1266/76/108		1728/46/108
Goodness of fit on F^2	1.181		1.091
Final R indices ($I > 2\sigma(I)$)	$R_1 = 0.0466$, $wR_2 = 0.0975$		$R_1 = 0.0380$, $wR_2 = 0.0992$
R indices (all data)	$R_1 = 0.0523$, $wR_2 = 0.1073$		$R_1 = 0.0434$, $wR_2 = 0.1027$
Extinction coefficient	0.0019(4)		0.0028(5)
Largest diff. peak and hole	0.591 and -0.562 e Å^{-3}		0.869 and -1.188 e Å^{-3}

cations. The ferroelectric phase transition is visible as a clear discontinuity in the spin–lattice relaxation time (^{1}H T_1) pointing to the distinct change in the reorientational dynamics of the organic cations [6, 7].

DMABA undergoes a ferro–paraelectric phase transition at 164 K (mixed type) and another structural phase transition/rearrangement at $\sim$228 K [8]. In spite of the fact that the ferroelectric properties in DMABA were discovered in 1987 the crystal structure of the paraelectric phase has not been solved to date. ^{1}H NMR studies [9] on DMABA indicate the change in the motional state of dimethylammonium cations around the ferro–paraelectric transition at 164 K. It is interesting that a clear anomaly in $T_{1\rho}$ was also found at 228 K in this crystal.

The dielectric relaxation studies on DMABA up to 500 MHz have shown that the dielectric behaviour of the crystal in the vicinity of the ferro–paraelectric phase transition is well described by the Cole–Cole formula with the critical slowing down of the relaxation frequency [4]. Also a trace of another, higher frequency dielectric contribution has been found, which could not be investigated in the frequency range accessible in the study.

The aim of this study is to determine the structure of the paraelectric high temperature phase and study the nature of the anomaly/rearrangement at 228 K in $[(CH_3)_2NH_2]_3Sb_2Br_9$. The properties of the low and high frequency contributions of the dielectric relaxation (up to 10 GHz) in the vicinity of the ferroelectric phase transition at 164 K are determined.

2. Experimental details

Single crystals of DMABA were grown by slow evaporation from aqueous solution containing 3:2 mole fraction of $[NH(CH_3)_2]$ and Sb_2O_3 with concentrated HBr. The synthesized
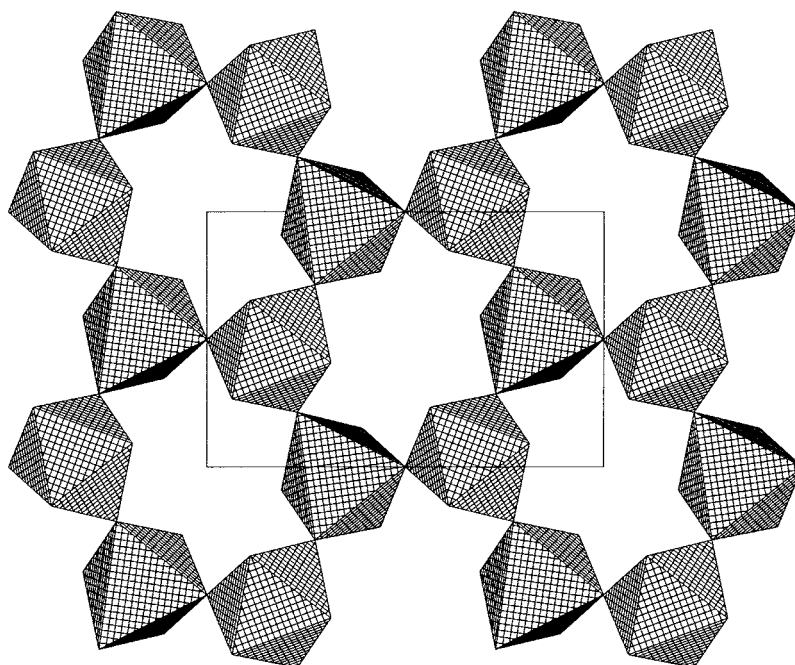
Figure 1. The layer structure of DMABA in the *b*–*c* plane in the polyhedral representation.

compound was purified by repeated crystallizations. Yellow and transparent crystals in the form of hexagonal plates were obtained.

Data for structure determination were collected on a KM-4 KUMA diffractometer with Mo Kα radiation ($\lambda = 0.710\,73$ Å, graphite monochromator). Lattice parameters were refined from setting angles of 27 reflections in the $17° < 2\theta < 31°$ range. The ω–θ scan technique (scan speed 0.02–0.15 s^{-1}, scan width 1.0) was used. Two control reflections measured after an interval of 50 reflections show that the intensity variation was negligible. Lorentz, polarization and absorption corrections were applied. The SHELXL97 program was used for all the structure calculations [10]. The summary of the measurement parameters is presented in table 1. A list of the calculated and observed structure factors may be obtained from the authors on request.

The thermal expansion studies were carried out on a single crystal of DMABA using a KM 4 diffractometer. The lattice parameters were refined from setting angles of 25 reflections in the $18° < 2\theta < 25°$ range. The temperature was controlled using an Oxford cryosystem attachment.

The dielectric measurements were made on discs of 2–4 mm diameter and 0.5–1 mm thickness with the symmetry axis of the disc parallel to the ferroelectric *a* axis in DMABA. Dielectric measurements in the frequency range 100 Hz–1 MHz were made using an HP 4575A *LCR* meter. In the frequency range 1 MHz–10 GHz the complex dielectric permittivity was estimated measuring the reflection factor in the coaxial line using HP 4191A and HP8510B impedance analysers. The equipment assembled and used many times for dielectric measurements of various ferroelectrics and other crystals at the University of Saarbrücken has been described elsewhere [11, 12]. The temperature during the spectrum collection was stabilized with accuracy of at least 0.005 K.
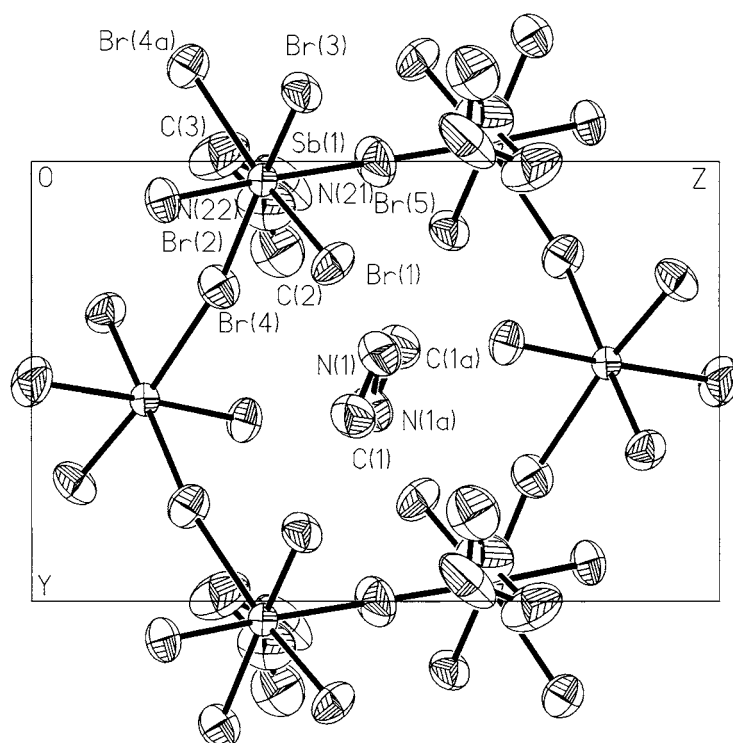
Figure 2. Projection of the crystal structure of DMABA at 293 K in the *b*-c plane. Thermal ellipsoids are at 50% probability.

3. Results

3.1. Crystal structure

We have collected two data sets at 293 and 180 K. At both temperatures the symmetry of the crystal lattice is monoclinic $P2_1/c$. Table 2 shows atomic co-ordinates of DMABA at 180 and 293 K. In the high temperature phase the crystal structure of DMABA is isomorphous with the chlorine analogue DMACA. The anionic sublattice is composed of distorted $SbBr_6$ octahedra connected with each other by corners, in such a way that three bromines are bridging and three are terminal. The octahedra form corrugated layers similar in appearance to a honeycomb, which are parallel to the *b–c* plane (figure 1). The Sb–Br bond lengths fall into two clearly defined ranges, 2.578(2) to 2.631(2) Å for terminal bromines and 3.007(2)–3.166(2) Å for bridging ones at 293 K (table 3). At 180 K the Sb–Br bond lengths slightly change from 0.004(2) Å for Sb(1)–Br(1) to 0.036(2) Å for Sb(1)–Br(4). It should be noted that the largest changes, to Br(3) and Br(4), are associated with the changes in the hydrogen bonding scheme (table 4). The Br–Sb–Br angles for bonds *cis* one to the other vary from 85.9(1) to 98.0(1)° at 293 K and they also slightly change on cooling to 180 K from 0(1) to 0.9(1)°; again the largest changes are associated with Br(3) and Br(4). The differences in bond lengths and angles indicate that those octahedra are significantly distorted.

There are two crystallographically independent dimethylammonium cations in the crystal structure. One is located in voids inside the polyanionic layers, the other one between the layers (figure 2). Cations are connected to the anionic sublattice by the N–H · · · Br hydrogen

Table 2. Atomic coordinates ($\times 10^4$) and equivalent isotropic displacement parameters ($\text{Å}^2 \times 10^3$) for DMABA. U_{eq} is defined as one third of the trace of the orthogonalized U_{ij} tensor.

	x	y	z	U_{eq}
293 K				
Sb(1)	1710(1)	417(1)	3360(1)	48(1)
Br(1)	3035(2)	2312(2)	4379(1)	85(1)
Br(2)	3015(2)	881(2)	1909(1)	78(1)
Br(3)	3505(2)	−1560(2)	3925(1)	78(1)
Br(4)	−161(2)	2846(2)	2724(1)	81(1)
Br(5)	0	0	5000	105(1)
N(1)	460(3)	4360(4)	5070(2)	108(10)
C(1)	890(2)	5790(3)	4676(14)	109(7)
N(21)	3360(5)	5480(5)	1326(17)	126(10)
N(22)	2600(4)	5990(6)	1590(4)	135(15)
C(2)	3690(3)	7010(5)	1429(17)	128(7)
C(3)	3090(3)	4870(6)	2360(19)	141(8)
180 K				
Sb(1)	1717(1)	449(1)	3346(1)	25(1)
Br(1)	3071(1)	2345(1)	4368(1)	58(1)
Br(2)	3033(1)	916(1)	1879(1)	47(1)
Br(3)	3577(1)	−1522(1)	3912(1)	46(1)
Br(4)	−161(1)	2861(1)	2724(1)	51(1)
Br(5)	0	0	5000	89(1)
N(1)	448(19)	4334(18)	4977(14)	71(6)
C(1)	869(14)	5832(14)	4666(8)	69(4)
N(21)	3331(16)	5607(15)	1319(9)	87(5)
N(22)	3630(6)	6380(3)	2289(19)	90(2)
C(2)	3615(16)	7147(15)	1394(10)	84(4)
C(3)	3101(17)	4855(17)	2255(13)	112(6)

bonds. The geometrical parameters of hydrogen bonds are presented in table 4. Both cations are disordered at 293 and 180 K. The model of disorder of the N(1) cation is shown in figure 3. The occupancy factor of the N(1) atom is equal to 0.5 and does not change between 293 and 180 K. The second cation is also split between two positions, N(21) and N(22). At 293 K the occupancy factors for N(21) and N(22) are equal to 0.66 and 0.34, while at 180 K to 0.8 and 0.2, respectively. At 293 K the plane of N(21), C(2) and C(3) forms 108° to the plane defined by N(22), C(2) and C(3). At 180 K the position of N(22) changes in such a way that N(21), N(22), C(2) and C(3) are almost coplanar (the angle between the N(22), C(2), C(3) and N(21), N(22), C(2) planes is equal to 18°). This is accompanied by changes in the hydrogen bonding scheme involving N(22) (table 4). Since this cation is in the general position these changes do not lead to changes in symmetry of the lattice. It should be noted, however, that changes in occupancy factors and the position of N(22) atom imply that the disorder is dynamical in nature and may contribute to the anomaly of electric permittivity observed at $T_c = 164$ K and below.

In figure 4(a) and 4(b) is presented the temperature dependence of the lattice parameters for DMABA between 100 and 290 K. One clear anomaly is visible at ∼164 K corresponding to the temperature of ferro–paraelectric phase transition. The thermal changes of lattice parameters are qualitatively similar to those found in DMACA, except for the *b* parameter, which in DMACA increased monotonically in the high temperature phase and started to decrease just below T_c [5]. In DMABA close to T_c its temperature characteristic along the *b* axis is exactly

Table 3. Selected bond lengths [Å] and angles [°] for DMABA.

	293 K	180 K
Sb(1)–Br(1)	2.578(2)	2.574(1)
Sb(1)–Br(2)	2.608(2)	2.614(1)
Sb(1)–Br(3)	2.631(2)	2.648(1)
Sb(1)–Br(4)	3.007(2)	2.970(1)
Sb(1)–Br(4′)	3.166(2)	3.153(1)
Sb(1)–Br(5)	3.076(2)	3.072(1)
Br(1)–Sb(1)–Br(2)	94.9(1)	95.0(1)
Br(1)–Sb(1)–Br(3)	89.3(1)	88.7(1)
Br(1)–Sb(1)–Br(4)	87.0(1)	86.8(1)
Br(1)–Sb(1)–Br(4′)	174.0(1)	173.4(1)
Br(1)–Sb(1)–Br(5)	86.1(1)	86.3(1)
Br(2)–Sb(1)–Br(3)	89.6(1)	89.1(1)
Br(2)–Sb(1)–Br(4)	88.3(1)	88.3(1)
Br(2)–Sb(1)–Br(4′)	88.6(1)	88.8(1)
Br(2)–Sb(1)–Br(5)	176.1(1)	176.1(1)
Br(3)–Sb(1)–Br(4)	175.6(1)	174.7(1)
Br(3)–Sb(1)–Br(4′)	85.9(1)	85.9(1)
Br(3)–Sb(1)–Br(5)	94.6(1)	94.6(1)
Br(4)–Sb(1)–Br(4′)	98.0(1)	98.8(1)
Br(4)–Sb(1)–Br(5)	87.6(1)	88.1(1)
Br(4′)–Sb(1)–Br(5)	90.7(1)	90.3(1)

Symmetry transformations used to generate equivalent atoms:
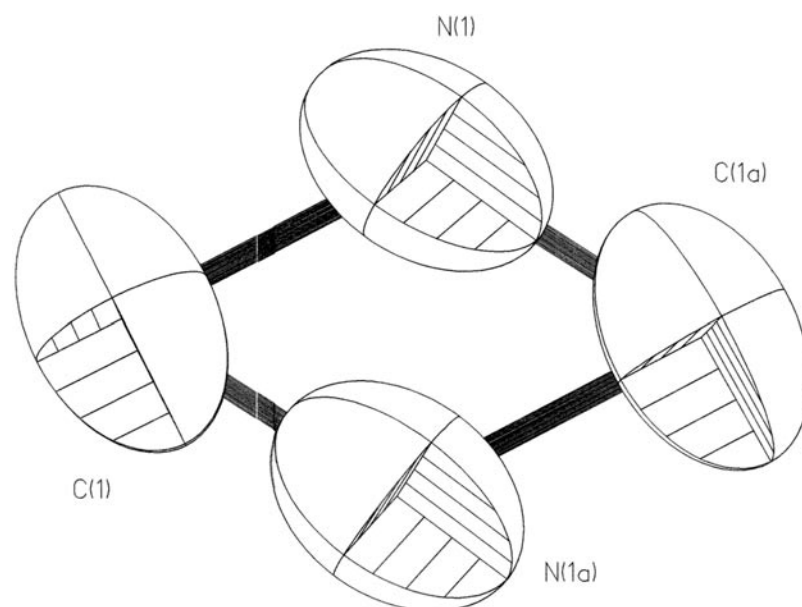′ $-x, y - 0.5, 0.5 - z$.

Figure 3. Disordered DMA(1) cation located at the symmetry centre at 293 K. Thermal ellipsoids are at 50% probability.

Table 4. Hydrogen bonds for DMABA.

	N–H	H···Br	N···Br	N–H···Br
293 K				
N(1)–H(1A)···Br(2′)	0.9	2.66(2)	3.545(2)	166(2)
N(21)–H(21A)···Br(3″)	0.9	2.82(2)	3.686(2)	161(2)
N(21)–H(21B)···Br(5‴)	0.9	2.87(2)	3.755(2)	167(2)
N(22)–H(22A)···Br(4⁗)	0.9	2.32(2)	3.214(2)	176(2)
N(22)–H(22B)···Br(5⁗′)	0.9	2.70(2)	3.441(2)	141(2)
180 K				
N(1)–H(1A)···Br(2′)	0.9	2.72(1)	3.578(1)	160(1)
N(1)–H(1B)···Br(1)	0.9	2.69(1)	3.525(1)	155(1)
N(21)–H(21A)···Br(3″)	0.9	2.81(1)	3.651(1)	156(1)
N(21)–H(21B)···Br(5‴)	0.9	2.79(1)	3.679(1)	169(1)
N(22)–H(22A)···Br(3⁗)	0.9	2.31(1)	3.033(1)	163(1)
N(22)–H(22B)···Br(2‴)	0.9	2.52(1)	3.407(1)	170(1)

Symmetry transformations used to generate equivalent atoms:
′ $-x, 0.5-y, 0.5+z$
″ $x, 0.5+y, z-0.5$
‴ $1-x, y+0.5, 0.5-z$
⁗ $-x, y+0.5, 0.5-z$
⁗′ $x, 1+y, z$.

opposite. The b parameter decreases in the high temperature phase and starts to increase just below $T_c = 164$ K.

3.2. Dielectric studies

Figure 5 displays the temperature dependence of the real part of the complex dielectric permittivity measured along the a-axis at 1 kHz. The following conclusions can be drawn from these results:

(i) the critical dielectric anomaly near the ferroelectric phase transition is observed in a very narrow temperature range of about 20 K (160–180 K); the critical relaxator contributes to the permittivity only in this small temperature range;
(ii) above about 80 K another dielectric contribution can be clearly distinguished (see inset);
(iii) the postulated phase transition at 228 K does not (or very slightly) influence the dielectric behaviour of DMABA in the a direction.

The results of dielectric relaxation measurements performed in the frequency range of 1 MHz–10 GHz are shown in figures 6(a)–(c) for three temperatures above the ferro–paraelectric phase transition (180, 170 and 166 K) and one below the phase transition (at 162 K, figure 6(d)). The results are presented as the frequency dependence of both parts of the permittivity (ε', ε'') and Cole–Cole plots (ε'' as a function of ε'—insets). The experimental data can be well fitted with the formula, being a sum of the Cole–Cole response of two independent relaxators I and II,

$$\varepsilon^* = \varepsilon_\infty + \frac{\varepsilon_{s1} - \varepsilon_{s2}}{1 + (\mathrm{j}f/f_{r1})^{1-h_1}} + \frac{\varepsilon_{s2} - \varepsilon_\infty}{1 + (\mathrm{j}f/f_{r2})^{1-h_2}} \tag{1}$$

where f denotes the measuring frequency, f_{r1} and f_{r2} the relaxation frequency of the relaxators I and II, $\varepsilon_{s1} - \varepsilon_{s2} = \Delta\varepsilon_1$ and $\varepsilon_{s2} - \varepsilon_\infty = \Delta\varepsilon_2$ the amplitudes of both relaxators and h_1 and h_2 parameters characterizing the relaxation time distribution.
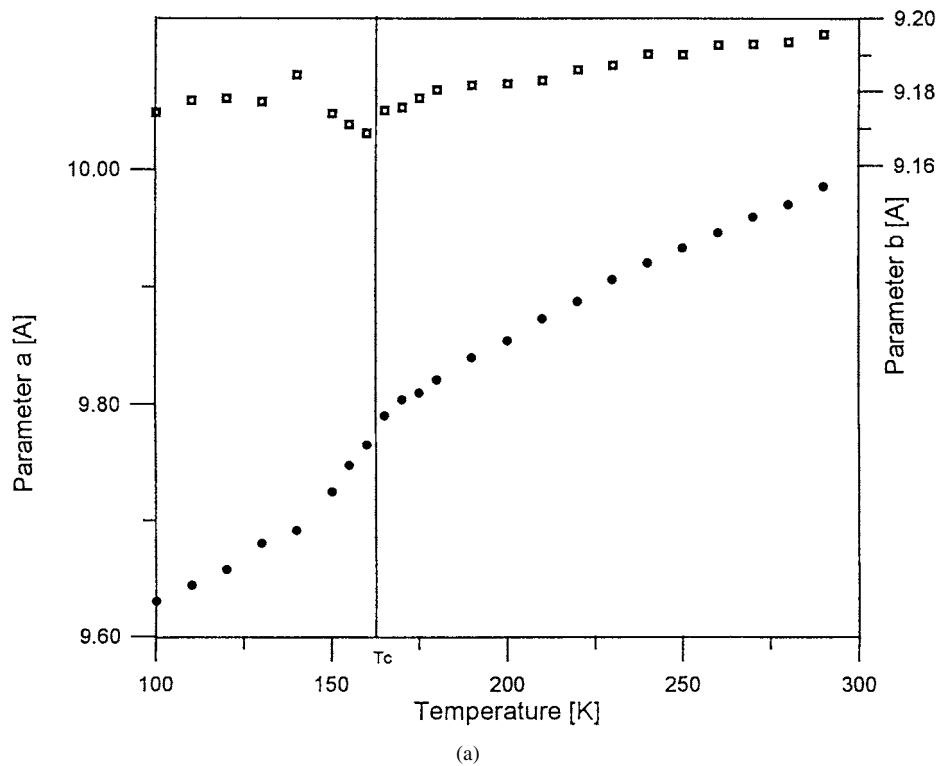
Figure 4. (a) Temperature dependence of the *a* (●) and *b* (□) lattice parameters and (b) temperature dependence of the *c* (◇) parameter and beta angle (+) for DMABA.

From the presented sequence of results it is clearly seen that the high frequency relaxator II exists in the entire temperature range measured, above and below the ferroelectric transition. Approaching the transition temperature from above the low frequency relaxator (I) appears. Its amplitude ($\Delta\varepsilon_1$) increases with decreasing temperature, reaching a maximum value at T_c, and then the increment rapidly vanishes just below the transition.

The temperature dependences of the amplitudes of both relaxators can be seen in figure 7 where the temperature dependences of parameters ε_∞, ε_{s1} and ε_{s2} are presented.

Our results for the low frequency relaxator I are very similar to those reported previously [4]; its amplitude $\Delta\varepsilon_1$ fulfils the Curie–Weiss law and the relaxation frequency f_{r1} slows critically at the transition point $T_c = 164$ K. The high frequency relaxator is thermally activated. Its characteristic frequency f_{r2} fulfils the Arrhenius dependence (figure 8) with a very small activation energy of 0.045 eV. A singularity in the $f_{r2}(1/T)$ dependence found at T_c seems to have sample dependence. In some samples it is much less pronounced or does not exist at all.

From the presented results one can conclude that the dynamic dielectric behaviour of DMABA in the ferroelectric *a* direction of the crystal is determined by the properties of two relaxators: a low frequency ($\sim$1 MHz at T_c) relaxator I and a high frequency ($\sim$5 GHz) relaxator II. The dielectric contribution of the relaxator I prevails near the paraelectric–ferroelectric phase transition $T_c = 164$ K. The relaxator I slows down critically at T_c and its amplitude fulfils the Curie–Weiss law (at least in the paraelectric phase). The activation energy found from the temperature dependence of the microscopic relaxation time of this relaxator was estimated
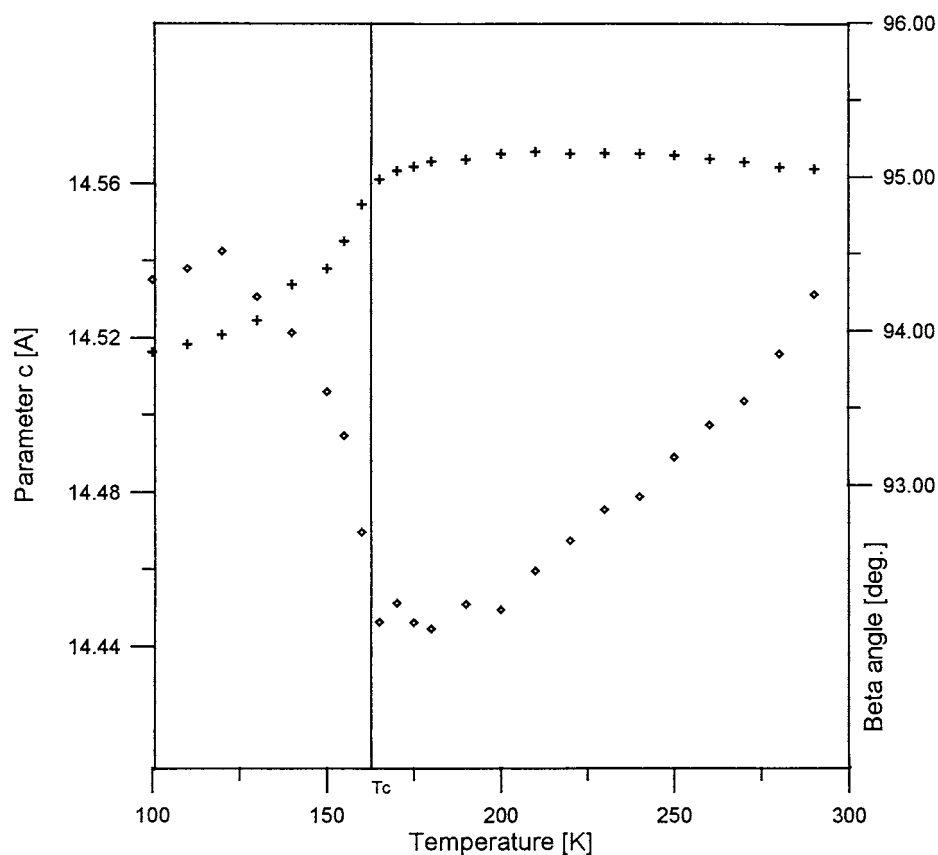
Figure 4. (Continued)

to be 0.23 eV [4]. The high frequency relaxator II contributes to the permittivity from about 80 K. Its amplitude increases monotonically with temperature without pronounced singularity at T_c. It is thermally activated with a very small activation energy of 0.04 eV, similar for both phases.

4. General discussion

The dynamic dielectric properties of several ferroelectric crystals of the group of halogenoantimonates(III) and bismuthates(III) namely $[(CH_3)_2NH_2]_3Sb_2Cl_9$ (DMACA) [4], $[(CH_3)_3NH]_3Sb_2Cl_9$ (TMACA) [13], $[CH_3NH_3]_5Bi_2Cl_{11}$ [14] and $[CH_3NH_3]_5Bi_2Br_{11}$ [12] together with DMABA studied here show several similarities. In each of them one can distinguish at least two ferroelectric relaxators of which one behaves critically, whereas the other one is thermally activated. Their presence was explained by at least two types of crystallographically non-equivalent organic cation, possessing different surroundings in the crystal lattice and consequently different activation energies of the reorientational motions. They constitute two types of cationic sublattice, each of which gives a different contribution to the spontaneous polarization and the complex electric permittivity in the high and low temperature phases.
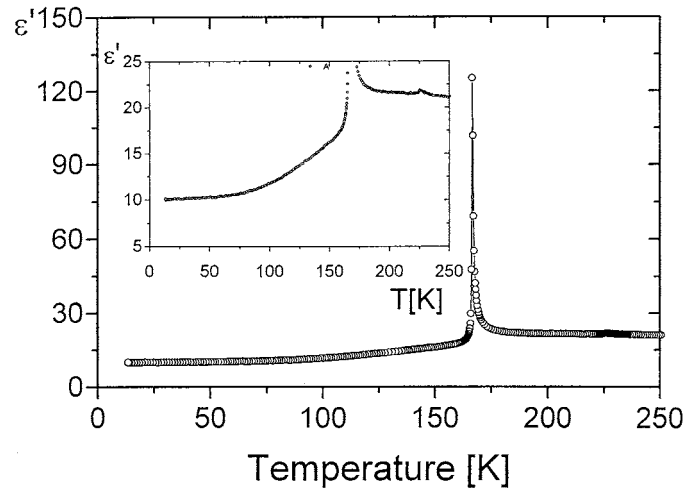
Figure 5. Temperature dependence of the real part (ε'_a) of the complex electric permittivity in the *a* direction measured at 1 kHz. The inset shows the same on a larger scale.
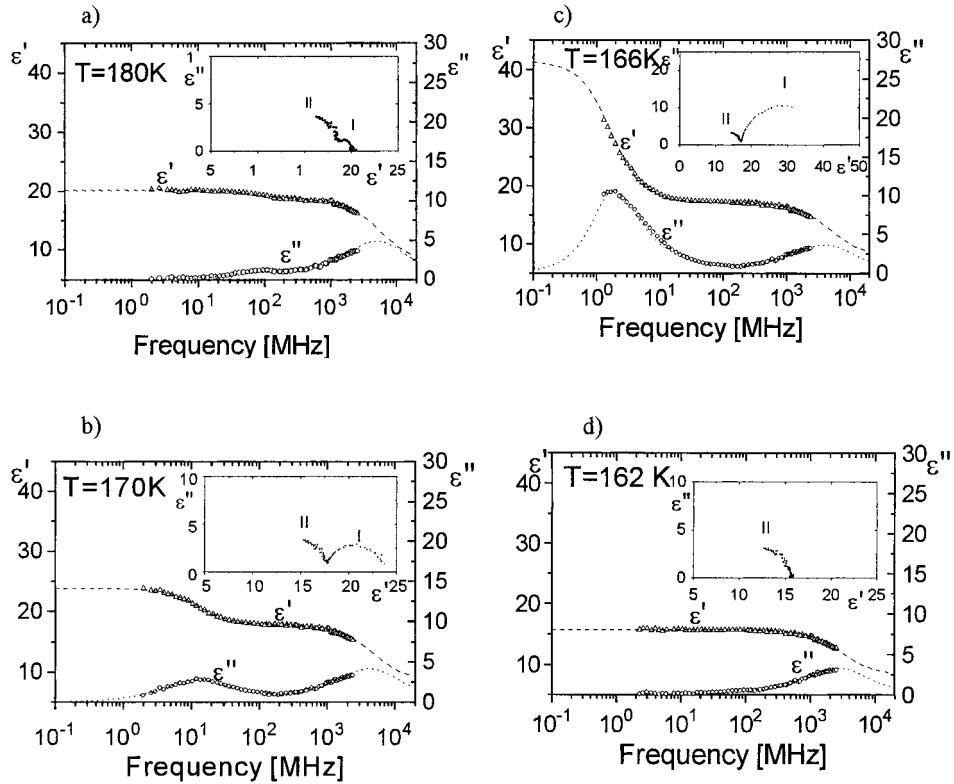

Figure 6. Frequency dependences of real (ε') and imaginary (ε'') parts of the complex electric permittivity and Cole–Cole plots for various temperatures above (a), (b) and (c) and below (d) the ferro–paraelectric phase transition. Lines were obtained using the formula (1). The fitting parameters (see equation (1)) at 180, 170, 166 and 162 K are the following: f_{r_1} [MHz]: 74, 12.5, 1.6, —; f_{r_2} [GHz]: 5.21, 4.46, 4.39, 2.83; h_1: 0.028, 0.041, 0.096, —; h_2: 0.092, 0.115, 0.132, 0.10, respectively.
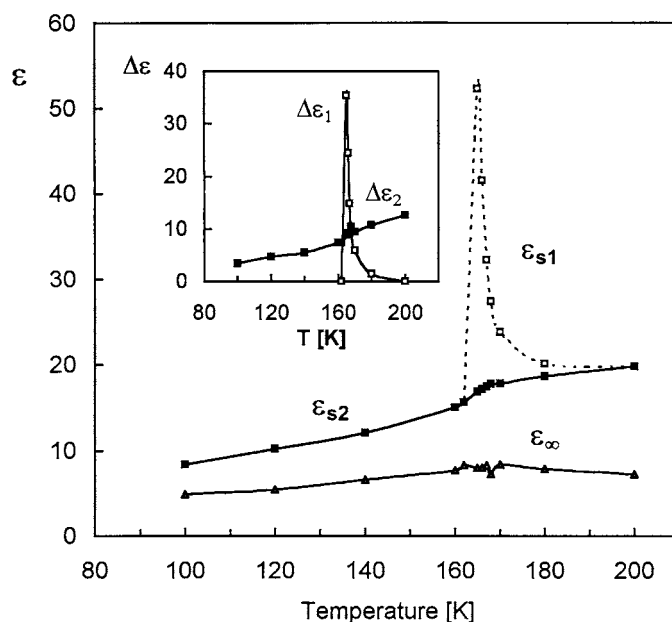
Figure 7. Temperature dependences of the limit values of the permittivity ε_∞, ε_{s1} and ε_{s2}. The inset shows the temperature dependence of amplitudes of both relaxators, $\Delta\varepsilon_1$, $\Delta\varepsilon_2$.
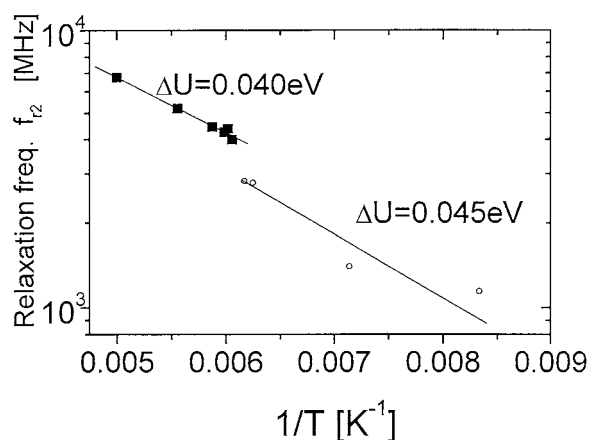

Figure 8. Arrhenius plot for the relaxation frequency f_{r2} of the high frequency relaxator.

The characteristic feature of the ferroelectric crystals possessing the $R_3Sb_2X_9$ stoichiometry (DMACA, DMABA and TMACA) is the presence of a two dimensional layer structure of polyanions. DMACA [15] and DMABA crystallize in the paraelectric phase in monoclinic $P2_1/c$ symmetry having two inequivalent disordered dimethylammonium cations. The ferroelectric phase in TMACA and DMACA is associated with the monoclinic Pc symmetry [4, 16]. In the low temperature ferroelectric phase of DMACA there are three independent cations in the crystal structure: one ordered inside the polyanionic vacancies and two others, ordered and disordered between the polyanionic layers. In TMACA the situation is similar: the position of atoms of trimethylammonium cations have not been split; however one

of the cations also possesses much higher thermal ellipsoids then the others indicating much larger thermal motions. The ferroelectric properties in the case of DMACA were explained by the ordering of the DMA cation located inside the polyanionic cavities. Since DMACA and DMABA are isomorphous at room temperature we may expect closely related dynamical properties of the cationic sublattices in the paraelectric phase.

In DMABA it seems that the DMA(1) type of cation located at the centre of symmetry is responsible for the critical slowing down of the macroscopic relaxation time and gives a basic contribution to the spontaneous polarization P_s below T_c of 164 K. The second DMA(2) type of cation, which is characterized by a change of the occupancy factor with temperature is distributed between two equivalent positions in the high temperature paraelectric phase. This type of cation is associated with a high frequency relaxator which does not show critical properties.

One should also notice the significant differences in the static dielectric properties of DMACA and DMABA which involve (i) differences in the anisotropy of dielectric properties. In DMACA the maximum of the dielectric permittivity close to T_c is shown along the *c* axis, whereas in DMABA along the *a* axis. In the same directions are observed the maximum values of the spontaneous polarization, (ii) significantly different temperature characteristics of the spontaneous polarization. In DMABA a change in the sign of the spontaneous polarization observed a few degrees below T_c [8]. This effect may be explained by at least two contributions to the spontaneous polarization coming from two different cationic sublattices. The presence of the high frequency relaxators both in the high and the low temperature phases confirms the possibility of the dynamical behaviour of the DMA(2) cation and as a consequence its contribution to the spontaneous polarization in the ferroelectric phase.

The effects presented above have their source probably in the different deformation of the anionic sublattices, which changes with temperature mostly at T_c. That is also clearly reflected in the different dilatation of both crystals along the *b* direction. In the case of a non-deformed polyanionic sublattice, we would expect two different values of lengths of Sb–Br contacts: one characteristic for bonds involving terminal bromines and the other one for those involving bridging ones. In the case of DMACA [5] deformation of lengths of Sb–Cl bonds is the result of formation of weak N–H$\cdots$Cl hydrogen bonds, which displace Cl$^-$ atoms in the direction of the positive charge located on N$^+$. This results in changes in lengths of the Sb–Cl bonds up to a maximum value of 0.047 Å for terminal chlorines and 0.160 Å for the bridging ones at 298 K in the high temperature paraelectric phase. In the case of DMABA at 293 K, those deformations are somewhat smaller and equal a maximum of 0.028 Å for terminal and 0.083 Å for the bridging bromines. This probably comes from the fact that N-H$\cdots$Br hydrogen bonds are much weaker and the energy required to displace Br atoms in the direction of cations is higher. It should be noted that on decreasing temperature those deformations increase up to 0.042 Å for terminal and 0.070 Å for bridging bonds, respectively.

Preliminary x-ray diffraction studies in the low temperature ferroelectric phase show, in contrast to the situation in DMACA [11] and TMACA [16] a change of symmetry to the triclinic $P1$ space group. This leads to ferroelastic twinning and as a consequence prevents us from solving the structure in the ferroelectric phase. It should be noted that in the case of the chlorine analogue DMACA the transformation leads to the monoclinic Pc space group [5].

One of the aims of this paper was to explain the anomaly of physical properties observed at 228 K in DMABA [3, 9]. The present x-ray diffraction studies showed that this effect is not associated with a change of the symmetry of the crystal. It was shown, however, that at $\sim$228 K there takes place a structure rearrangement, which is associated with the change of the disorder of one of the structurally independent cations: that located in between the polyanionic layers. This rearrangement is associated with a change in the hydrogen bonding scheme to

N(22). The lack of the phase transition comes from the fact that the DMA(2) cation is located in the general position in the crystal lattice and as a result its rearrangement does not lead to the change of the symmetry of the crystal.

5. Conclusions

The crystal structure of ferroelectric $[NH_2(CH_3)_2]_3Sb_2Br_9$ (DMABA) has been determined at 293 K and 180 K in the paraelectric phase. It is isomorphous with the chlorine analogue DMACA. In the crystal lattice of DMABA one can distinguish two types of crystallographically inequivalent, disordered dimethylammonium cation (DMA): one of them located inside the polyanionic cavities and the other one in between the layers. Only the former is responsible for the ferroelectricity in DMABA.

Different physical anomalies observed around 228 K must result from the rearrangement of the structure. The x-ray diffraction studies confirm the distinct change in the hydrogen bonding scheme involving N(22) between 293 K and 180 K. That confirms the change in the dynamic state of the second type of cation, which does not lead to a change in symmetry. Therefore the possibility of phase transition in DMABA at 228 K is precluded.

The dynamic dielectric behaviour in DMABA around the ferro–paraelectric transition at 164 K is determined by the presence of two independent relaxators, strictly connected with two types of crystallographically independent DMA cation. The low frequency relaxator exhibits a critical slowing down close to T_c, whereas the high frequency one is only thermally activated. In contrast to DMACA, exhibiting a ferro–paraelectric transition of pure second order type at 243 K, in the case of DMABA the dielectric dispersion studies indicate the first order character of the ferroelectric phase transition at 164 K.

References

[1] Jakubas R and Sobczyk L 1990 *Phase Transitions* **20** 163
[2] Sobczyk L, Jakubas R and Zaleski J 1997 *Pol. J. Chem.* **71** 265
[3] Jakubas R, Sobczyk L and Matuszewski J 1987 *Ferroelectrics* **74** 339
[4] Bator G and Jakubas R 1995 *Phys. Status Solidi* a **147** 591
[5] Zaleski J and Pietraszko A 1996 *Acta Crystallogr.* B **52** 287
[6] Jagadeesh B, Rajan P K, Venu K and Sastry V S S 1994 *Solid State Commun.* **91** 843
[7] Medycki W, Piślewski N and Jakubas R 1996 *Ferroelectrics* **185** 205
[8] Jakubas R, Mróz J, Francois P and Lefebvre J 1995 *Ferroelectrics* **173** 221
[9] Idziak S and Jakubas R 1987 *Solid State Commun.* **67** 173
[10] Sheldrick G M 1997 *SHELXL97 Program for the Refinement of Crystal Structures*
[11] Luther G 1973 *Phys. Status Solidi* a **20** 227
[12] Pawlaczyk Cz, Planta K, Bruch Ch, Stephan J and Unruh H G 1992 *J. Phys.: Condens. Matter* **4** 2687
[13] Sobiestianskas R, Czapla Z and Grigas J 1992 *Phys. Status Solidi* a **130** K69
[14] Pawlaczyk Cz, Jakubas R, Planta K, Bruch Ch and Unruh H G 1992 *J. Phys.: Condens. Matter* **4** 2695
[15] Gdaniec M, Kosturkiewicz Z, Jakubas R and Sobczyk L 1988 *Ferroelectrics* **77** 31
[16] Kallel A and Bats J W 1985 *Acta Crystallogr.* C **41** 1022